AFRL-PR-WP-TR-2002-2083

DEMONSTRATION OF TEMPERATURE MEASUREMENT ON A CURVED SURFACE USING THERMOGRAPHIC PHOSPHORS

Jamie Ervin (University of Dayton)
Mechanical and Aerospace Engineering Department
University of Dayton
Dayton, OH

Christopher Murawski
Charles MacArthur

Turbine Branch (AFRL/PRTC)
Turbine Engine Division
Propulsion Directorate
Air Force Research Laboratory, Air Force Materiel Command
WPAFB, OH 45433-7251

Minking Chyu (Carnegie-Mellon University)
David Bizzak (Carnegie-Mellon University)

Mechanical Engineering Department
Carnegie-Mellon University
Pittsburgh, PA

20021107 019

MAY 2002

Final Report for 28 May 1991 – 30 September 1992

**PROPULSION DIRECTORATE
AIR FORCE RESEARCH LABORATORY
AIR FORCE MATERIEL COMMAND
WRIGHT-PATTERSON AIR FORCE BASE, OH 45433-7251**

NOTICE

USING GOVERNMENT DRAWINGS, SPECIFICATIONS, OR OTHER DATA INCLUDED IN THIS DOCUMENT FOR ANY PURPOSE OTHER THAN GOVERNMENT PROCUREMENT DOES NOT IN ANY WAY OBLIGATE THE US GOVERNMENT. THE FACT THAT THE GOVERNMENT FORMULATED OR SUPPLIED THE DRAWINGS, SPECIFICATIONS, OR OTHER DATA DOES NOT LICENSE THE HOLDER OR ANY OTHER PERSON OR CORPORATION; OR CONVEY ANY RIGHTS OR PERMISSION TO MANUFACTURE, USE, OR SELL ANY PATENTED INVENTION THAT MAY RELATE TO THEM.
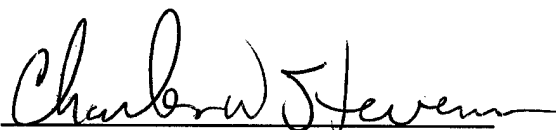
THIS REPORT IS RELEASABLE TO THE NATIONAL TECHNICAL INFORMATION SERVICE (NTIS). AT NTIS, IT WILL BE AVAILABLE TO THE GENERAL PUBLIC, INCLUDING FOREIGN NATIONS.

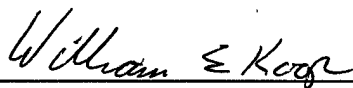THIS TECHNICAL REPORT HAS BEEN REVIEWED AND IS APPROVED FOR PUBLICATION.

DR. CHRIS G. MURAWSKI
Program Manager, Turbine Branch
Turbine Engine Division
Propulsion Directorate

CHARLES W. STEVENS
Chief, Turbine Branch
Turbine Engine Division
Propulsion Directorate

WILLIAM E. KOOP
Chief, Turbine Engine Division
Propulsion Directorate

Do not return copies of this report unless contractual obligations or notice on a specific document requires its return.

REPORT DOCUMENTATION PAGE

The public reporting burden for this collection of information is estimated to average 1 hour per response, including the time for reviewing instructions, searching existing data sources, searching existing data sources, gathering and maintaining the data needed, and completing and reviewing the collection of information. Send comments regarding this burden estimate or any other aspect of this collection of information, including suggestions for reducing this burden, to Department of Defense, Washington Headquarters Services, Directorate for Information Operations and Reports (0704-0188), 1215 Jefferson Davis Highway, Suite 1204, Arlington, VA 22202-4302. Respondents should be aware that notwithstanding any other provision of law, no person shall be subject to any penalty for failing to comply with a collection of information if it does not display a currently valid OMB control number. **PLEASE DO NOT RETURN YOUR FORM TO THE ABOVE ADDRESS.**

1. REPORT DATE (DD-MM-YY)	2. REPORT TYPE	3. DATES COVERED (From - To)
May 2002	Final	05/28/1991 – 09/30/1992

4. TITLE AND SUBTITLE	5a. CONTRACT NUMBER
DEMONSTRATION OF TEMPERATURE MEASUREMENT ON A CURVED SURFACE USING THERMOGRAPHIC PHOSPHORS	In-house

5b. GRANT NUMBER

5c. PROGRAM ELEMENT NUMBER
61101F

6. AUTHOR(S)

Jamie Ervin (UD)
Christopher Murawski (AFRL/PRTC)
Charles MacArthur (AFRL/PRTC)
Minking Chyu (CMU)
David Bizzak (CMU)

5d. PROJECT NUMBER
ILIR

5e. TASK NUMBER
P0

5f. WORK UNIT NUMBER
09

7. PERFORMING ORGANIZATION NAME(S) AND ADDRESS(ES)

Mechanical and Aerospace Engineering Department University of Dayton Dayton, OH	Turbine Branch (AFRL/PRTC) Turbine Engine Division Propulsion Directorate Air Force Research Laboratory, Air Force Materiel Command WPAFB, OH 45433-7251	Mechanical Engineering Department Carnegie-Mellon University Pittsburgh, PA

8. PERFORMING ORGANIZATION REPORT NUMBER

AFRL-PR-WP-TR-2002-2083

9. SPONSORING/MONITORING AGENCY NAME(S) AND ADDRESS(ES)

Propulsion Directorate
Air Force Research Laboratory
Air Force Materiel Command
Wright-Patterson Air Force Base, OH 45433-7251

10. SPONSORING/MONITORING AGENCY ACRONYM(S)

AFRL/PRTC

11. SPONSORING/MONITORING AGENCY REPORT NUMBER(S)

AFRL-PR-WP-TR-2002-2083

12. DISTRIBUTION/AVAILABILITY STATEMENT
Approved for public release; distribution is unlimited.

13. SUPPLEMENTARY NOTES

14. ABSTRACT

An optical technique for surface temperature measurement based on the fluorescent emission of rare-earth ion-doped phosphors was demonstrated in an experiment with a heated cylinder in cross flow. In this experiment, a uniform heat flux is imposed by applying a constant voltage across the thin stainless-steel cylinder surface to produce surface temperatures between 24 °C and 55 °C. The fluorescent emission of a thermographic phosphor, lanthanum oxysulfide doped with europium (La_2O_2S:$Eu+3$) deposited on the surface, was recorded to determine the temperature distribution at the curved surface. When excited by ultraviolet radiation, the phosphor emits a spectrum containing certain emission lines, and the intensities of these vary with temperature.

15. SUBJECT TERMS
instrumentation, temperature measurement, thermographic phosphors, cylinder

16. SECURITY CLASSIFICATION OF:			17. LIMITATION OF ABSTRACT:	18. NUMBER OF PAGES	19a. NAME OF RESPONSIBLE PERSON (Monitor)
a. REPORT Unclassified	b. ABSTRACT Unclassified	c. THIS PAGE Unclassified	SAR	30	Christopher Murawski 19b. TELEPHONE NUMBER (Include Area Code) (937) 255-7277

HES&S 31-15093-1

ABSTRACT

An optical technique for surface temperature measurement based on the fluorescent emission of rare-earth ion-doped phosphors was demonstrated in an experiment with a heated cylinder in cross flow. In this experiment, a uniform heat flux is imposed by applying a constant voltage across the thin stainless-steel cylinder surface to produce surface temperatures between 24°C and 55°C. The fluorescent emission of a thermographic phosphor, lanthanum oxysulfide doped with europium ($La_2O_2S:Eu^{+3}$) deposited on the surface, was recorded to determine the temperature distribution at the curved surface. When excited by ultraviolet radiation, the phosphor emits a spectrum containing certain emission lines, and the intensities of these vary with temperature. For a single temperature-sensitive line, the ratio of the intensity at a reference temperature to intensity at different temperatures were correlated as a function of surface temperature. The use of intensity ratio correlations avoids complications due to geometric (viewing angle) effects.

Digitized images of the cylinder permitted calculation of surface temperatures and local Nusselt numbers. A comparison of surface temperature measurements from calibrated thermocouples to those from the phosphor technique indicate that the uncertainty in the surface temperature determined with the phosphor is ± 1.1°C.

INTRODUCTION

Thermographic phosphors are ceramics consisting of rare-earth oxides, vanadates, phosphates, or oxysulfides in which a small amount of the original rare-earth constituent is replaced with a different rare-earth element (a dopant). Electron transitions of stimulated dopant atoms cause fluorescence in the phosphor; this fluorescence is modified by temperature-dependent, dopant self-interaction and by other complex interactions involving the original rare-earth material [1, 2, 3, 4]. When excited,

1

thermographic phosphors emit a spectrum characterized by unique emission lines, and both the intensity and fluorescence lifetime of these lines vary with temperature. With ultraviolet irradiation, these phosphors fluoresce at distinct wavelengths. As a result, three methods can be used for thermometry with thermographic phosphors. The first correlates the lifetime of the fluorescent emission with temperature, the second relies on the relationship between the emission amplitude of two spectral lines with temperature, and the third depends on the emission amplitude of a single spectral line with temperature. A typical fluorescent spectrum consists of many lines. The intensity of some of these lines varies significantly with temperature; the intensity of others does not. A ratio of the intensity of a temperature-sensitive line to a temperature-insensitive one (as in the second method) or to the same temperature-sensitive line at a single reference temperature (as in the third method) is preferable to making an absolute intensity measurement because of the practical difficulties of photometric measurements in most fluid flow situations.

Determination of temperature using the fluorescent lifetime method is described elsewhere [4, 5, 6, 7, 8, 9, 10, 11]. In a review paper, Dowell [4] presents current theories about the change in fluorescence with temperature, demonstrating that fluorescent amplitude and ratios of amplitudes of different spectral lines depend on temperature. He states that precise amplitude measurements traceable to metrological standards are difficult. Nevertheless, for many engineering applications, the correlation of ratios of amplitudes of emitted spectral lines may be completely adequate for practical temperature measurement. Furthermore, temperature determination by correlation of fluorescent lifetime with temperature for nonisothermal surfaces to date has only provided single-point measurements rather than two-dimensional field measurement, which is the objective of the present work.

2

Studies involving the use of ratios of intensities are relatively few. Goss et al. [12] demonstrated the feasibility of thermographic phosphors to measure the surface temperature of combusting rocket propellent. Noel et al. [13] have shown analytically the ability to remove the spatially distributed effects of both illumination and emission intensities with a ratio method which uses two different wavelengths. The ratio of two images, each at a different wavelength, is independent of the spatial distribution of both illumination and fluorescent emission. This ratio was also shown to be proportional to the surface temperature of the test object. Chyu and Bizzak [14] and Bizzak and Chyu [2] developed a laser-induced fluorescence thermal imaging system capable of accurate ($\pm$ 0.5°C), two-dimensional temperature measurement on a relatively small, flat surface using two different $La_2O_2S:Eu^{+3}$ emission lines. An image-intensified camera was gated for an effective "shutter speed" of either 35 or 40 μsec, and integrated fluorescent emmissions were accumulated over several laser pulses. Taliaferro et al. [15] found temperature calibration curves in terms of ratios of images for lanthanum oxysulfide or yttrium oxysulfide airbrushed on a flat aluminum substrate. These calibration curves resulted from using the image recorded at room temperature as the reference image to form ratios with images at higher temperatures.

The intent of the current research is to measure surface temperatures by correlating fluorescent amplitude ratio with temperature. In contrast to previous work, the present study uses a large curved surface in a defined flow. For a single temperature-sensitive wavelength, ratios were formed between an image at the reference temperature and images at higher temperatures. The potential for two-dimensional temperature measurement based on the fluorescent emission of europium-doped lanthanum oxysulfide ($La_2O_2S:Eu^{+3}$) was examined by obtaining the local Nusselt number (Nu) about the midplane of a cylinder in cross flow with an imposed uniform heat flux.

3

EXPERIMENTAL APPARATUS

Figure 1 illustrates the experimental arrangement. A phosphor-coated cylinder with a height equal to that of the wind tunnel test section was electrically heated. The ultraviolet lamp-induced fluorescent emission of the phosphor (which was detected by the CCD video camera) and the video images obtained were digitized and stored on a computer for later processing. The individual components of Fig. 1 are described in detail below.

The cylinder shown in Fig. 2 was fabricated from a stainless-steel sheet measuring 15.2 cm (6 in.) x 27.9 cm (11 in.) x 0.05 mm (0.002 in.). The stainless-steel sheet was wrapped around two 8.9 cm (3.5 in.) diameter brass disks separated by 8.9 cm (3.5 in.) diameter cylinders made of polyurethane insulation. This insulation prevented natural convection within the cylinder that, if permitted, would affect the local heat transfer from the outer cylinder surface during the experiment. Lanthanum oxysulfide doped with a 0.1% molar concentration of europium was dissolved in an organic binder (Sperex VHT115-clear) and sprayed uniformly with an extra fine airbrush to form a thin coating (0.3 mm thick) on the steel sheet. Preliminary testing showed that this coating thickness resulted in a uniform fluorescence signal and negligible thermal resistance. The thin thermographic phosphor coating did not significantly alter the macroscopic surface profile. The coated sheet was cured in a furnace to ensure adherence of the phosphor to the stainless-steel and to remove the volatile components of the binder. The midplane of the inner cylinder surface was instrumented with 30 gage (0.025 cm or 0.010 in. diameter) type J thermocouples which were referenced to a calibrated electronic ice point (Kaye Instruments Model 270-360). Additional thermocouples were located above and below the midplane as shown in Fig. 3, which shows the stainless-steel sheet with the thermocouple locations marked before it is wrapped around the insulation. The thermocouple leads passed through

holes drilled in the insulation and the upper brass disk. The surface thermocouples were bonded to the inner steel surface with thermally conductive epoxy with an area of attachment of approximately 0.32 ± 0.04 cm ($1/8 \pm 1/64$ in.) x 0.32 ± 0.04 cm ($1/8 \pm 1/64$ in.). These thermocouples were located (within $\pm 3°$) at $0°$, $22.5°$, $45°$, $90°$, $135°$, $-45°$, and $-90°$ with respect to the front stagnation region of the cylinder. The outer cylinder surface was marked at these locations for viewing by the video camera. For symmetric flow conditions about the cylinder, the temperatures at angular locations of $-45°$ and $45°$ or at $-90°$ and $90°$ were expected to be the same, and the quality of this agreement corroborated the thermocouple readings. Machined aluminum clamps held the stainless-steel sheet in contact with the brass disks, which also served as power terminals.

A uniform heat flux was impressed on the cylinder by maintaining a constant AC voltage across the steel sheet, and a rheostat in combination with an isolation transformer was used to adjust the heat flux level. Voltage measurements (known within ± 0.1 mV) across the cylinder and across a calibrated shunt (0.000667 ± 0.00002 Ω), placed in series with the cylinder and transformer, permitted calculation of the supplied power within ± 0.001 W/cm^2.

Excitation of the thermographic phosphor at a wavelength of 254 nm was provided by an ultraviolet lamp (UVP model UVG-54), which has a power density of 2.2 mW/cm^2 at a distance of 7.6 cm (3 in.) from the exposed surface. The lamp provided a nearly uniform irradiance over $165°$ of the cylinder surface with no surface heating as measured by the attached thermocouples.

The wind tunnel used in these experiments is shown in Fig. 4. The test section of the wind tunnel was 76.2 cm (30 in.) wide by 15.2 cm (6 in.) high. Honeycomb was placed at the inlet immediately before the test section to insure a well-defined mean velocity profile at the cylinder. For the range of flow velocity considered (4.7 m/s to 8.2 m/s), the vertical velocity profile was flat except near the upper

and lower wall boundary layers (which were on the order of 10 mm thick), as determined by a traverse of the test section with a pitot tube in combination with a water-filled micromanometer. The free-stream turbulence intensity in the test section of the wind tunnel was nominally 0.8%, as measured by a hot-wire anemometer. Two quartz windows 12.7 cm (5 in.) wide by 12.7 cm (5 in.) long were installed at the test section of the wind tunnel. One window passed ultraviolet radiation; the other permitted viewing by the video camera with nearly 165° of the cylinder within the camera view. A 3.7 kW (5 horsepower) blower drew air through the wind tunnel. Thermocouples were placed at four locations in the test section for measurement of the bulk fluid temperature for calculation of the local Nu.

The remaining components of the system provided the means to acquire and store images. The desired wavelength, 510 nm, of the fluorescent emission was selected by positioning a Pomfret 514-nm bandpass filter with a 9-nm bandwidth in a fixed filter holder directly before the 75-mm macro lens attached to the CCD video camera. The camera (Panasonic model WVD5100) required a minimum illumination of 7.5 lumens/m^2 and had a gain of up to +18 dB. A Data Translation DT2861 image acquisition card digitized the analog video signals, forming a 512-by-512 pixel array. Each pixel had an eight-bit intensity value, resulting in 256 gray scale levels. Attenuation from the bandpass filter required amplification of the optical signal passing through the filter, but internal amplification of the video signal by the camera introduced some noise. By time averaging 64 video frames for each acquired image, this noise was significantly reduced.

PROCEDURE

With the cylinder located in the wind tunnel prior to the forced flow tests, a calibration curve was determined from ratios of images acquired for different surface temperatures which were measured

6

using the calibrated surface thermocouples. Before calibration of the phosphor, all room lights were switched off to reduce possible noise effects in subsequent measurements, and the ultraviolet source was aligned with the cylinder, producing a nearly uniform fluorescent emission from the phosphor. After proper ultraviolet illumination was obtained, peripheral regions on the outer cylinder surface near the thermocouples were located using the alignment marks. These rectangular areas were 11 pixels wide by 25 pixels high, roughly corresponding to the area of contact of the thermocouple epoxy. During the initial calibration for small variations in the surface temperature, it was experimentally determined that temperature error decreased as the calculational area increased. Hence, this rectangle, in the given pixel dimensions was selected as the minimum imaging size.

A reference image of the fluorescing but unheated cylinder at the ambient temperature of 16°C (61°F) cylinder was digitized and used to determine all image ratios for both the initial calibration and actual testing under flow conditions. Images for calibration of the phosphor were captured at numerous temperatures between 16°C (61°F) and 49°C (120°F). The surface temperature was varied by changing the applied voltage across the foil cylinder surface. With the cylinder in nominally still air, a quasi-steady surface temperature was reached when the natural convection heat transfer became equal to the electrically generated surface heat flux. This temperature was measured using the surface-mounted thermocouples, with uncertainties of ± 0.3°C (0.5°F) over the temperature range of interest.

For each rectangle of pixels, ratios of pixel intensities were formed from the image digitized at the reference temperature together with images subsequently recorded at higher temperature levels. Statistical calculations for the mean pixel ratio and standard deviation were performed over the domain of these rectangles for a given surface temperature. Least squares curve fits relating the mean emission amplitude ratio to temperature for the rectangular regions were generated.

After the illuminated portion of the cylinder was calibrated, tests at Re_D of 3.2×10^4 and 5.7×10^4 for two different input power levels of 0.046 W/cm² and 0.072 W/cm² were performed resulting in a total of four forced-flow tests with laminar boundary layer flow around the forward portion of the cylinder. The first heat flux value was chosen to obtain a maximum surface temperature of about 31°C (88°F), while the peak temperature at the higher heat flux was nearly 36°C (97°F). Three images were obtained at each heat flux level to assess the repeatability of the results. The measured independent variables were the micromanometer pressure difference for velocity determination and mass flow rate adjustment, and the voltage differences across the shunt and cylinder for power determination. The dependent variables of the forced-flow experiments were the emission intensity from the excited phosphor, voltages from thermocouples attached to the inner cylinder surface, and voltages from the thermocouples used for the bulk fluid temperature determination.

The net heat flux to the air was calculated by subtracting estimated heat losses from the total supplied heat flux. The net heat flux, q", considered uniform since the change in resistivity with temperature of the steel foil is negligible in this instance, is given by:

$$q'' = V_{shu}V_{cyl} / (R_{shu} A_s) - q''_L \qquad (1)$$

where q''_L are estimated heat losses by radiation and conduction from the cylinder, V_{shu} is the voltage difference across the shunt, V_{cyl} is the voltage difference across the cylinder, R_{shu} is the shunt resistance, and A_s is the surface area.

Heat losses from the cylinder were estimated considering one-dimensional conduction through the cylinder insulation and the stainless-steel sheet. In the absence of forced flow, the measured average

8

temperature of the outer brass surface and the midplane together with values of the thermal conductivity provided estimates of conduction through the ends of the cylinder. For the temperatures considered together with tabulated values for the emissivity of stainless-steel [16], it was perceived that the radiative losses would be much smaller. With forced flow, the heat losses for a given average surface temperature are expected to be lower than those found with natural convection. Hence, estimates of the heat losses under actual test conditions are conservative.

Nu is calculated from:

$$Nu = q'' \, D \, / \, (K \, (T_s - T_\infty))$$ (2)

where D is the cylinder diameter, K is the thermal conductivity of the air, T_s is the local cylinder surface temperature, and T_∞ is the free-stream temperature.

RESULTS

During the calibration of intensity ratio with temperature, a mean and standard deviation of the pixel intensity ratios were calculated for each rectangle of pixels; the standard deviation was less than ten percent of the mean value. The intensity ratio at a given temperature was not completely independent of the illumination angle and emission angle for every illuminated location on the cylinder. Hence, a single calibration curve for a fixed illumination angle and a fixed viewing angle for mean intensity ratio as a function of temperature could not be applied everywhere on the cylinder. It was found that, for the present orientation of the ultraviolet lamp and camera, three regions ($5° < \theta < 30°$, $30° < \theta < 135°$, and $135° < \theta < 165°$) could each be represented by individual calibration curves for areas between the stagnation region and $180°$ from the stagnation region. The calibration was

extremely sensitive to movement of the 514-nm bandpass filter. During preliminary testing, manual removal and replacement of the optical filter resulted in mean intensity ratio values that varied widely for a given temperature and location on the cylinder surface. Spatially varying nonuniformities in the filter may have caused this. Sensitivity to movement of the bandpass filter was prevented by holding the filter in a rigid fixture for both calibration and measurement.

Noel et al. [13] derived an expression for the imaged distribution of photons as a separable function of excitation geometry, excitation amplitude, emission geometry, and a modulated temperature-dependent emission amplitude. When the ratio of two spectrally filtered images at known wavelengths are formed, the geometry dependence on object illumination and fluorescent emission cancel. Certainly, one would expect this also to be true for a ratio of images formed at the same wavelength but at different temperatures. However, here it is found that surface geometry may not be entirely neglected. In the derivation of the separable function, the surface was assumed to be a Lambertian emitter, and this may not be true for the real surface of this experiment.

Figure 5 shows the calibration curves for the lanthanum oxysulfide phosphor for the three surface regions noted in the preceding paragraphs. A polynomial curve fit calculated by the method of least squares for each of the three regions was used to determine the temperature in the range of interest, 23°C (74°F) to 36°C (97°F). For calibration, a reference image of the cylinder surface recorded at 16°C (61°F) was used to form a ratio with other subsequent images recorded at higher surface temperatures. Each symbol in the figure corresponds to the mean pixel ratio for a single calculation rectangle. Three other tests were performed under the same conditions for four different calculation rectangles (12 tests in all for each data point shown) in order to assess the repeatability of the technique. Also, Fig. 5 demonstrates that the sensitivity of temperature measurement varies with the temperature level. The

image ratio is most sensitive, for example, to changes in temperature between 19°C (66°F) and 21°C (70°F), and least sensitive to temperatures from 38°C (100°F) to 49°C (120°F). The smallest increment in temperature that could be measured was in the 19°C to 21°C range and was limited by the resolution of the thermocouples.

Figure 6 presents the temperature distribution about the midplane of the cylinder in cross flow for conditions of Re_D of 3.2×10^4 and a uniform heat flux of 0.046 W/cm^2. As expected, the temperature is a minimum near the stagnation region where Nu is greatest and a maximum near 90°, the location of flow separation. Temperatures measured with the present method were within ± 1.1°C (2°F) of the temperatures indicated by the calibrated thermocouples mounted on the cylinder, which served to verify the experimental procedure and calibration technique.

Figure 7 shows the variation of the dimensionless parameter, $Nu/(Re_D)^{1/2}$ with θ. Uncertainties in $Nu/(Re_D)^{1/2}$ estimated by the method of Kline and McClintock [17] were on the order of ± 15 percent, which arise largely from estimates of the heat loss. The curve for a Re_D of 3.2×10^4 in Fig. 7 is from Zukauskas [18] and corroborates the methodology used in determining Nu.

Potential sources of error in the temperature measurement using the present thermographic phosphor system include camera effects, nonuniformity of the phosphor coating, absorption of ultraviolet radiation by the binder, and the effect of nonuniform illumination. Camera effects, which include pixel-to-pixel variations, may be reduced by a flat-field correction as described in Chyu and Bizzak [19]. However, with the camera used in the present experiments, this correction was unnecessary. While the intensity of each emission line is affected by the uniformity of the phosphor, absorption of ultraviolet radiation by the binder, and the viewing angle, effects on the intensity ratio can be corrected by calibration of the test surface.

11

PRACTICAL SIGNIFICANCE

Thermocouples or resistance thermal devices which directly contact a surface are commonly used to evaluate heat transfer characteristics, but they may have serious disadvantages. Contacting sensors can conduct heat from the surface, changing the surface temperature. The test piece may require the machining of holes for installation of probes. Mounting numerous thermocouples on a gas turbine blade, for example, may disrupt the flow of cooling air within the intricate internal passages.

Infrared imaging and liquid crystal thermography may be preferred over thermocouple instrumentation, but these optical techniques have certain difficulties. Infrared imaging is feasible for objects at high temperature, but room temperature measurement is difficult because background thermal radiation cannot be adequately filtered, resulting in large measurement uncertainties. Liquid crystal thermography has a limited temperature range from -25°C to 250°C. Moreover, the active temperature range is relatively constricted and, as a consequence, liquid crystals may not be accurate in the presence of severe temperature gradients. However, the optical determination of the temperature distribution at a surface using a thermographic phosphor does not have any of the limitations noted above. Selection of the appropriate thermographic phosphor permits use of the present method under extreme thermal conditions, ranging from low cryogenic temperatures to high temperatures as in combustion [1, 12].

CONCLUSIONS

The thermographic phosphor method described can be used to determine two-dimensional surface temperatures for relatively large, curved surfaces with ±1.1°C uncertainty in temperature, and with a resolution here on the order of 0.3 cm (1/8 in.). The determination of the circumferential temperature

12

distribution and Nu on a heated cylinder in cross flow demonstrates the potential use of thermographic phosphors for heat transfer measurements.

Although somewhat less accurate than laser-induced fluorescence techniques which require a relatively expensive Nd:YAG laser, intensified camera, and additional collection optics (as in Chyu and Bizzak [2]). The single-wavelength method employed here is relatively inexpensive; and consequently, has greater potential for ordinary laboratory two-dimensional temperature measurements. In addition, the use of a single wavelength eliminates alignment difficulties associated with two-wavelength methods.

RECOMMENDATIONS

Alternative methods of coating surfaces with thermographic phosphors should be pursued. Currently, organic binders are used to maintain the phosphor layer. However, the resulting coating is fragile and the effect of ultraviolet absorption by the binder is difficult to quantify. In addition, at very high temperatures, organic binders may be impractical. Silicates have been used [2], but again the effects of ultraviolet absorption on temperature determination are difficult to assess. The low vapor pressure of the phosphors in many instances precludes vacuum deposition or sputtering.

ACKNOWLEDGEMENTS

13

NOMENCLATURE

A_s surface area, m^2

D   cylinder diameter, m

K   thermal conductivity, W / °C m

Nu   Nusselt number [$= q'' D / (K (T_s - T_\infty))$], dimensionless

q'' net heat flux, W / m^2

q''_L radiative and conductive losses, W / m^2

R   image ratio, dimensionless

R_{shu} shunt resistance, Ω

Re_D Reynolds number ($= UD/v$), dimensionless

T_s local surface temperature, °C

T_∞ free-stream temperature, °C

U   mean velocity of air, m / s

V_{cyl} voltage difference across cylinder, V

V_{shu} voltage difference across shunt, V

Greek

v kinematic viscosity, m^2 / s

θ angular coordinate from stagnation region, rad

REFERENCES

1. Fonger, W. H., and Struck, C. W., Eu^{+++} ^5D Resonance Quenching to the Charge-Transfer States in Y_2O_2S, La_2O_2S, and LaOCl, *J. Chem. Phys.*, **52**, 6364–6372, 1970.

2. Bizzak, D. J., and Chyu, M. K., Rare-Earth Phosphor Laser-Induced Fluorescence Thermal Imaging System, *Rev. Sci. Instrum.*, **65**, 102-107, 1994.

3. Hufner, S., *Optical Spectra of Rare Earth Compounds*, Academic Press, New York, 1978.

4. Dowell, L. J., Fluorescence Thermometry, *Appl. Mech. Rev.*, **45**, 253-260, 1992.

5. Izaguirre, F., Csanky, G., and Hawkins, G. F., Temperature Measurements with Micrometer Spatial Resolution, *Rev. Sci. Instrum.*, **62**, 1916-1920, 1991.

6. Allison, S. W., Monitoring Permanent Magnet Motor Heating with Phosphor Thermometry, *IEEE Trans. Inst. Meas.*, **37**, 637-641, 1988.

7. Gillies, G., Thermal Metrology for Gas Turbine Engines, *ASME International Gas Turbine and Aeroengine Tech. Rep.*, Atlanta, GA, pp. 88-89, 1987.

8. Grattan, K. T., and Palmer, A. W., Infrared Fluorescence "Decay-Time" Temperature Sensor, *Rev. Sci. Instrum.*, **56**, 1784-1787, 1985.

9. Grattan, K. T., Palmer, A. W., and Willson, C. A., A Miniaturized Microcomputer-Based Neodymium "Decay-Time" Temperature Sensor, *J. Phys. E.*, **20**, 1201-1205, 1987.

10. Cates, M. R., Laser-Induced Fluorescence of Europium-Doped Yttrium Oxide for Remote High-Temperature Thermometry, *Proc. Laser Inst. Am.*, **51**, 142-146, 1985.

11. Wickersheim, K., and Sun, M., Phosphors and Fiber Optics Remove Doubt about Difficult Temperature Measurements, *Res. and Dev.*, **27**, 114-119, 1985.

12. Goss, L. P., Smith, A. A., and Post, M. E., Surface Thermometry by Laser-Induced Fluorescence, *Rev. Sci. Instrum.*, **60**, 3702-3706, 1989.

13. Noel, B. W., Beshears, D. L., Borella, H. M., Sartory, W. K., Tobin, K. W., et al.., A 2-D Imaging Heat Flux Gauge, Los Alamos Report LA-12129-MS, July 1991.

14. Chyu, M. K., and Bizzak, D. J., Surface Temperature Measurement Using a Laser-Induced Fluorescence Thermal Imaging System, *ASME J. Heat Transfer*, **116**, 263-266, 1994.

15. Taliaferro, J. M., Allison, S. W., and Tobin, K. W., Two-Dimensional Thermography Using La_2O_2S:Eu and Y_2O_2S:Eu Thermal Phosphors, Oak Ridge National Laboratory Report ORNL/ATD-61, 1991.

16. Incropera, F. P., and DeWitt, D. P., *Introduction to Heat Transfer*, 2nd Ed., John Wiley and Sons, New York, 1990.

17. Kline, S. J., and McClintock, F. A., Describing Uncertainties in Single-Sample Experiments, *ASME Mech. Eng.*, **75**, 3-9, 1953.

15

18. Zukauskas, A., Heat Transfer from Tubes in Cross Flow, in *Advances in Heat Transfer*, J. P. Hartnett and T. F. Irvine, Jr., Eds., Vol. 8, pp. 93-161, Academic Press, New York, 1972.

19. Chyu, M. K., and Bizzak, D. J., Two-Dimensional Laser-Induced Fluorescence Temperature Measurement on a Rotating Surface, 29th National Heat Transfer Conference, Atlanta, GA, pp. 47-53, August 1993.
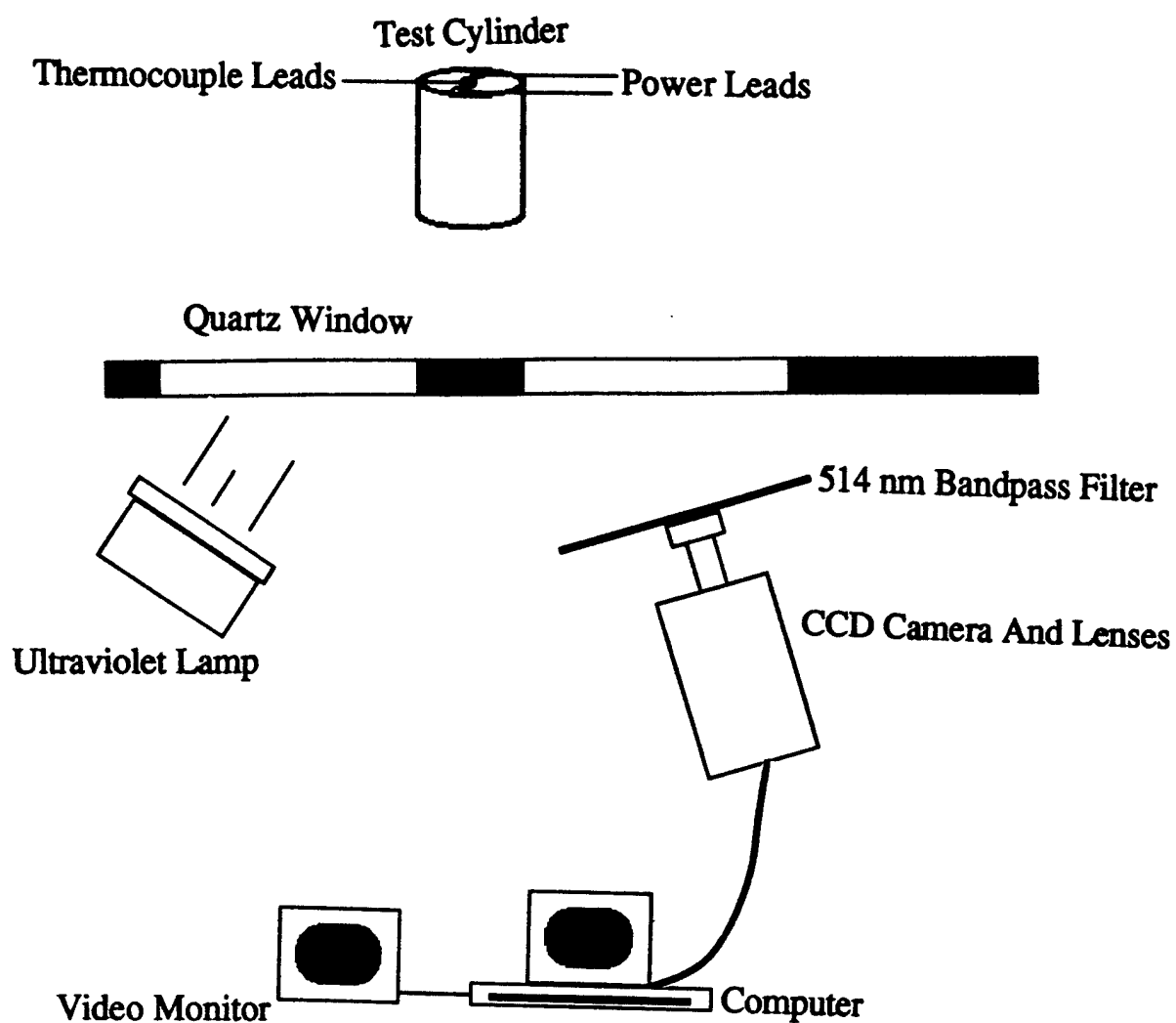
FIGURE LIST

Figure 1 Experimental Apparatus.
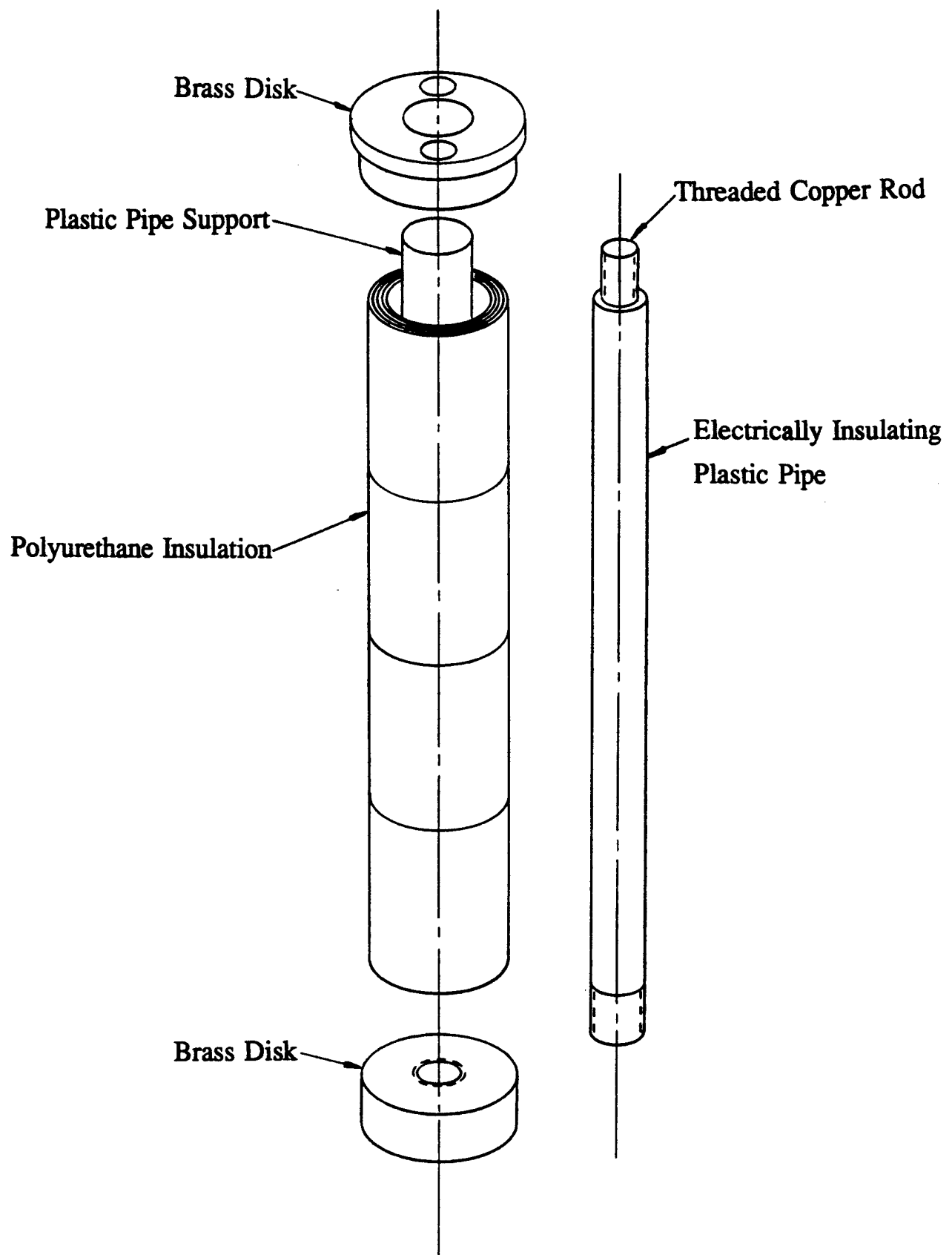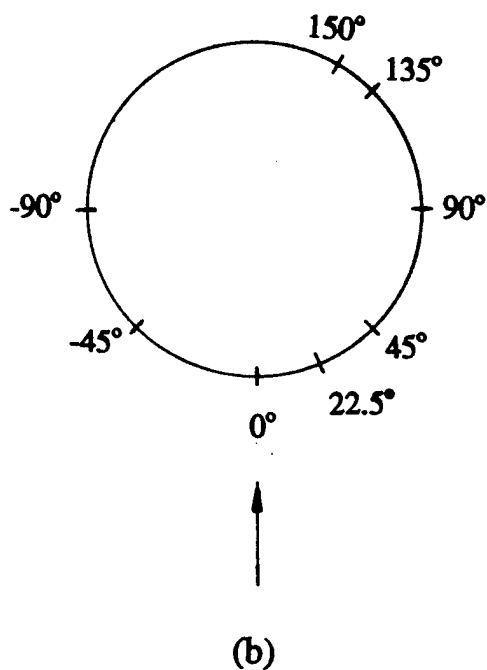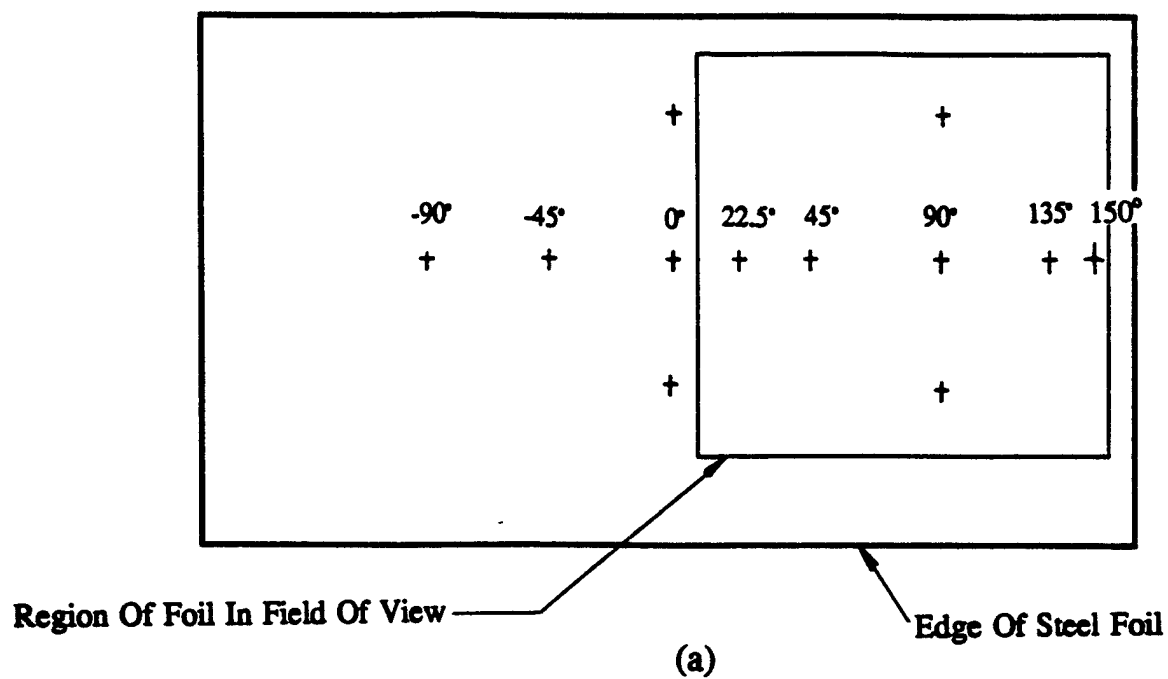
Figure 2 Assembly View Of Cylinder.

Figure 3 Views Of Thermocouple Locations On Stainless-Steel Sheet.
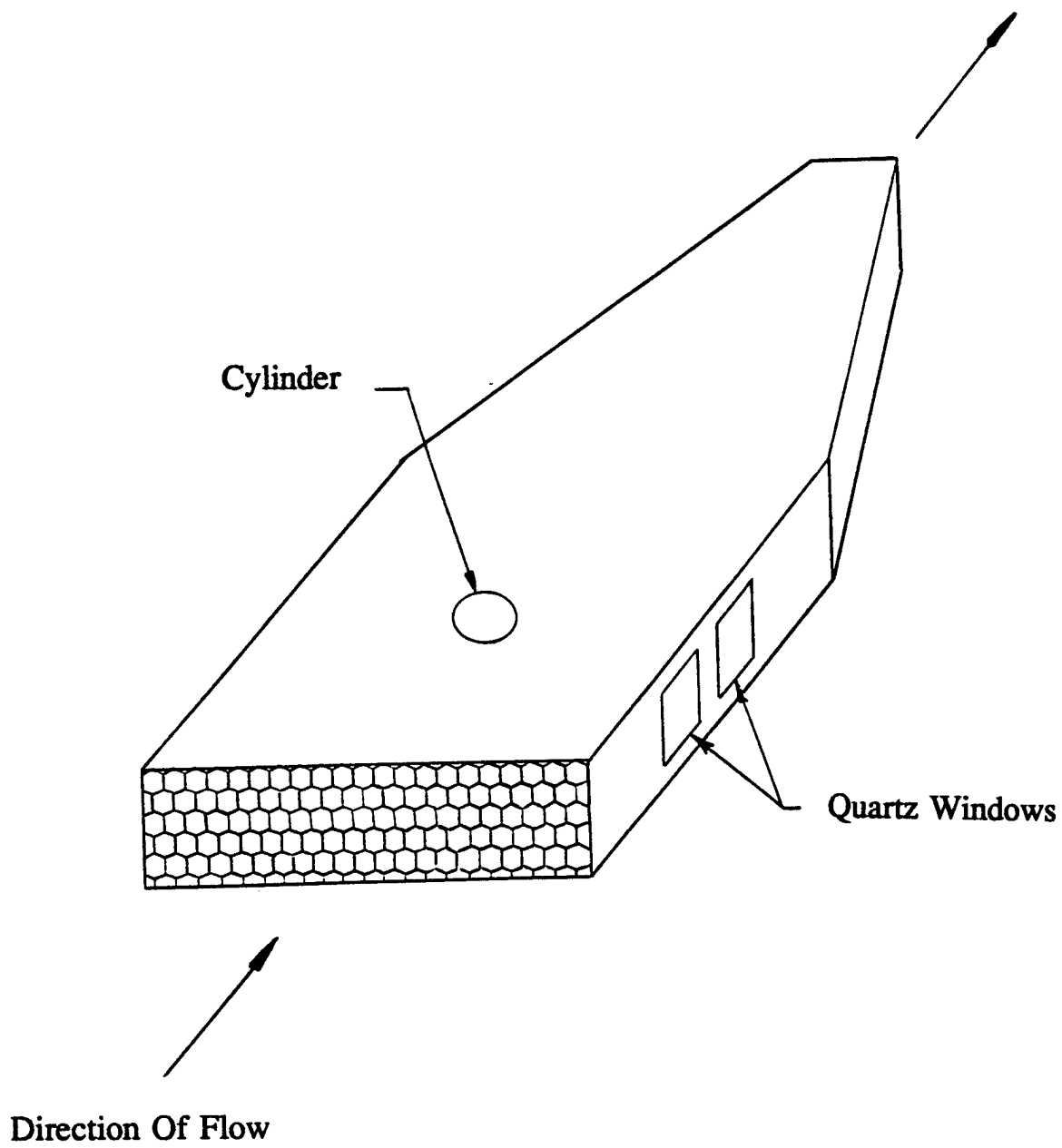(a) Unwrapped Sheet Surface. (b) Cylinder From Above.

Figure 4 Wind Tunnel.

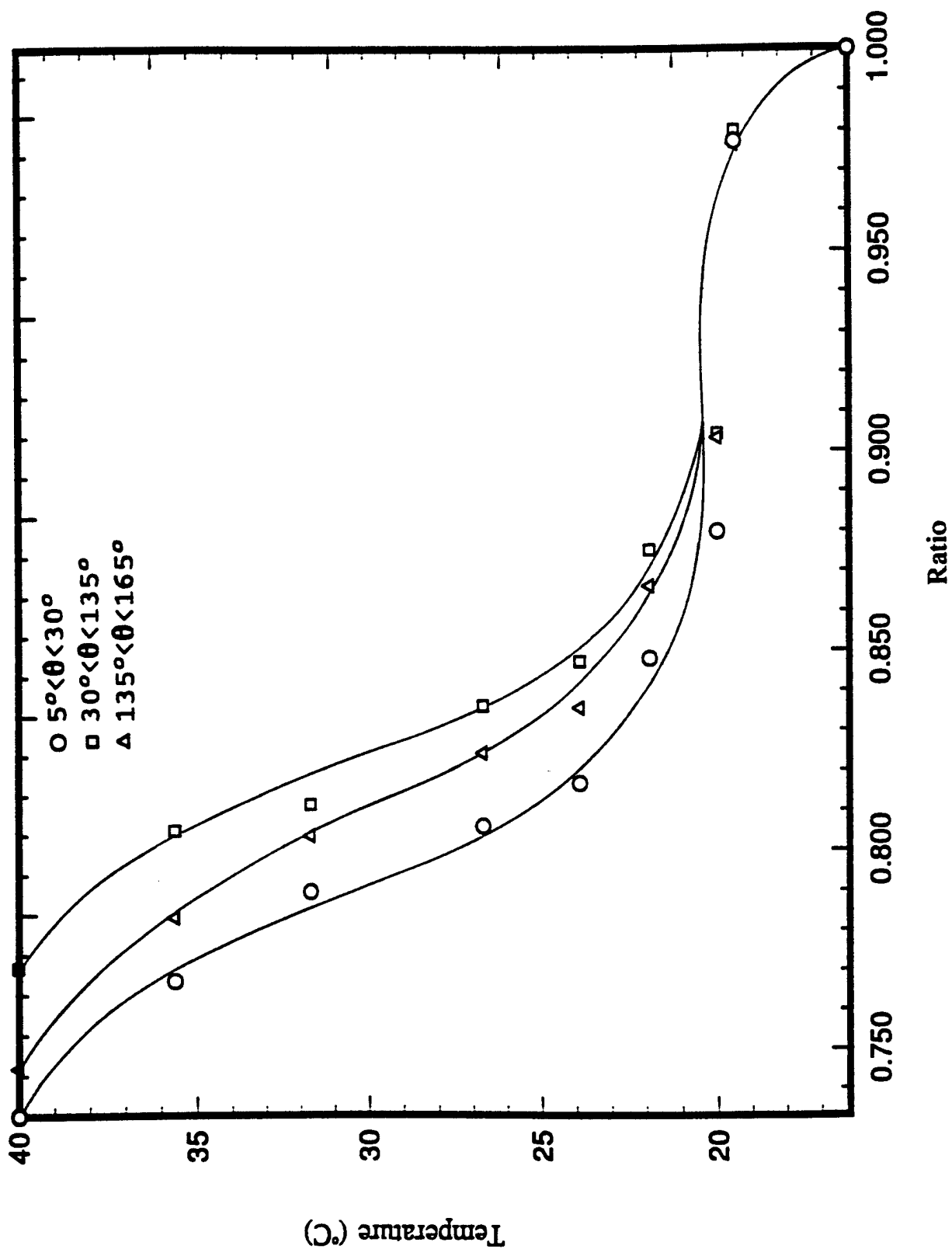Figure 5 Thermographic Phosphor Calibration Curves.

Figure 6 Midplane Temperature Distribution For Cylinder In Cross Flow.

Thermocouple Measurement
Phosphor Measurement

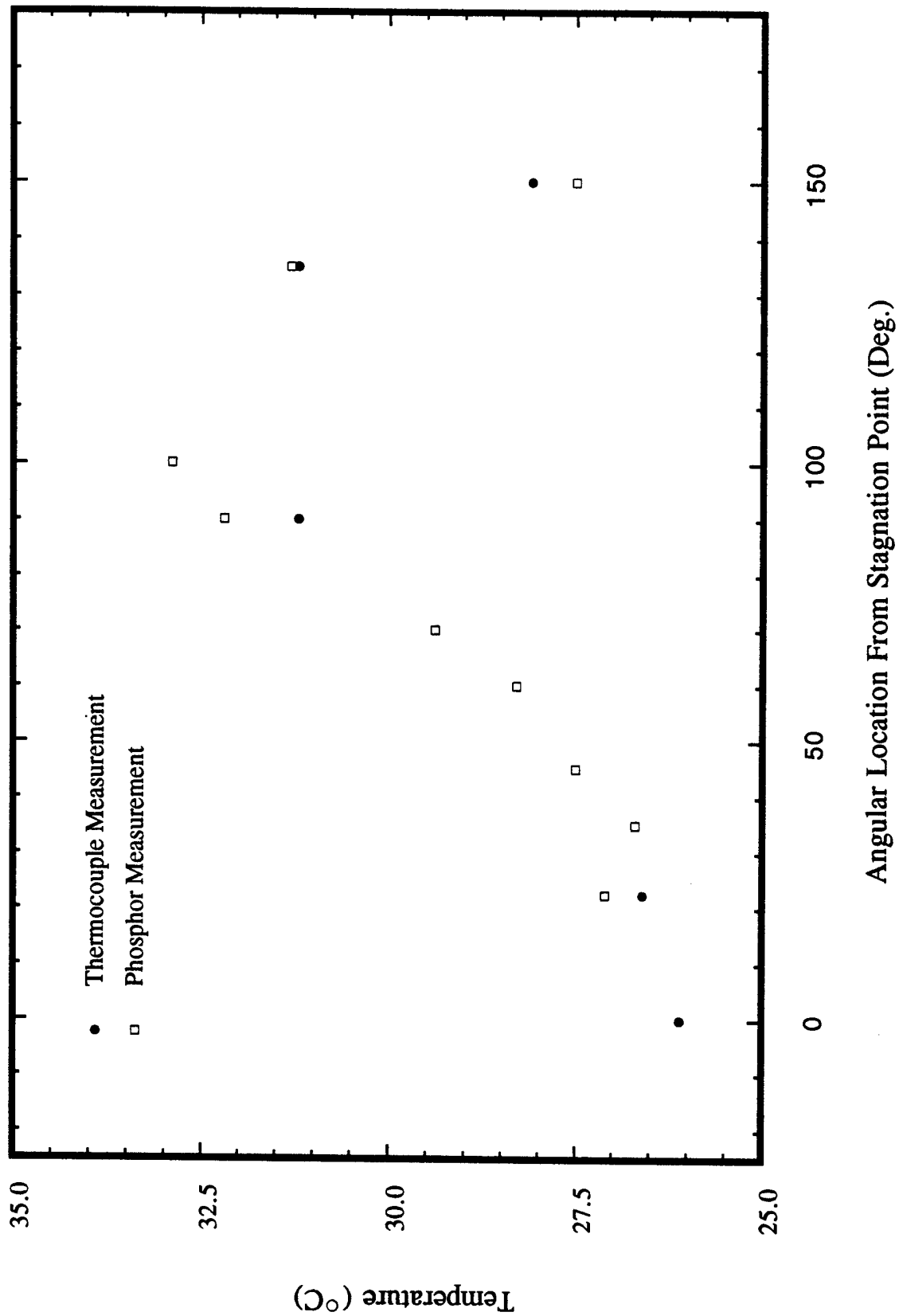Temperature (°C)

Angular Location From Stagnation Point (Deg.)

22

Figure 7 Angular Distribution Of Heat Transfer Parameter.

Thermographic Phosphor Measurement

Zukauskas (1972)

$Re_D = 32000$
$q'' = 0.046 \ W/cm^2$

$\dfrac{Nu}{\sqrt{Re_D}}$

θ Degrees From Stagnation Region